Tomographic Processing of Multi-Baseline P-Band SAR Data for Imaging of a Forested Area

Othmar Frey, Felix Morsdorf and Erich Meier
Remote Sensing Laboratories, University of Zurich, Switzerland
Email: ofrey@geo.unizh.ch

***Abstract*—Recently, various attempts have been undertaken to obtain information about the structure of forested areas from multi-baseline synthetic aperture radar data. Tomographic processing of such data has been demonstrated but the quality of the focused tomographic image is limited by several factors. In particular Fourier-based focusing methods are susceptible to irregular and sparse sampling, two problems, that are unavoidable in case of multi-pass, multi-baseline SAR data acquired by an airborne system. We propose a tomographic focusing method based on the time-domain back-projection algorithm, which maintains the geometric relationship between the original sensor positions and the imaged target and is therefore able to cope with irregular sampling without introducing any approximations with respect to the geometry. We assess the tomographic focusing quality with the help of the impulse response of simulated point targets and an in-scene corner reflector. And, in particular, preliminary results obtained with the newly acquired P-band tomographic data set consisting of eleven flight tracks are presented.**

I. Introduction

The common Fourier-based SAR processing algorithm, the SPECAN (SPECtral ANalysis) approach, which has been used in [1], requires that the synthetic aperture be sampled regularly and densely. In reality, the sampling spacing is not uniform in case of airborne SAR data of multiple acquisition paths, and the synthetic aperture in the normal direction is sampled sparsely. As a result the tomographic image is subject to defocusing, high side lobes and ambiguities in the normal direction. In order to overcome the ambiguity problem and to improve the resolution modern spectral estimation methods have been proposed as a substitute to spectral estimation by FFT. These methods include spectral estimation by the Capon method [2] and subspace-based spectral estimators such as the MUSIC algorithm [3] [4]. These methods replace the last step, the spectral estimation by FTT, but any geometric approximation made in a previous processing step is still present in the data. We adopt a time-domain back-projection (TDBP) processing technique, which maintains the entire three-dimensional geometric relationship between the exact sensor positions and the illuminated area while focusing the data. So, the key feature of the TDBP approach is an accurate handling of the complex geometry of multi-baseline airborne SAR data.

II. 3D focusing in the time-domain

In [5] an algorithm has been proposed which is based on single look complex images processed by the extended chirp scaling algorithm including aircraft motion compensation to a straight line. However, instead of focusing the data by deramping and spectral estimation, which would previously involve generating synthetic tracks and a regularization of the samples in the normal direction, a time-domain beamformer (TDB) was applied to focus the data in the third dimension. Every voxel within the volume is focused by a so-called *ad hoc* reference function as it is also known from time-domain back-projection processing. The focusing quality of the TDB approach was found to be superior to the SPECAN based algorithm presented in [1] for unevenly spaced baselines. But in spite of the fact that the TDB directly accounts for the irregular track distribution in normal direction it is still based on artificial, linearized flight tracks, which lie in parallel to each other and which do not represent the true geometry of the flight tracks. We aim at a complete processing in the time domain – after range compression – and focus the data by using the true geometry of the irregularly sampled tomographic acquisition pattern. A TDBP processor, which has been tested with airborne [6] and spaceborne SAR data [7], has been extended in order to work with a two-dimensional synthetic aperture. The main point is that the geometric relationship between every sensor position and the illuminated volume is maintained during focusing without introducing any geometric approximations. Following the derivations presented in [7] the back-projected signal s_k corresponding to the flight track k can be expressed as a function of the grid point $\vec{r}_i$:

$$s_k(\vec{r}_i) = \sum_{j=a_k(\vec{r}_i)}^{b_k(\vec{r}_i)} g_k(R_k, \vec{r}_{S_{jk}}) \cdot R_k \cdot \exp(i2k_c R_k) \ . \qquad (1)$$

$\vec{r}_i$	: position vector of the target
a_k, b_k	: indices of first, last azimuth position of the sensor within the synthetic aperture of the target position $\vec{r}_i$
$\vec{r}_{S_{jk}}$	: position vector of the sensor, $j \in [a_k, b_k]$
R_k	$= \lvert\vec{r}_i - \vec{r}_{S_{jk}}\rvert$: range distance
$g_k(.)$	: range-compressed signal of data track k
k_c	$= 2\pi f_c/c$: central wavenumber
f_c	: carrier frequency
c	: speed of light

By extending the coherent addition of the signal contributions to the normal direction the back-projected signal v is obtained,

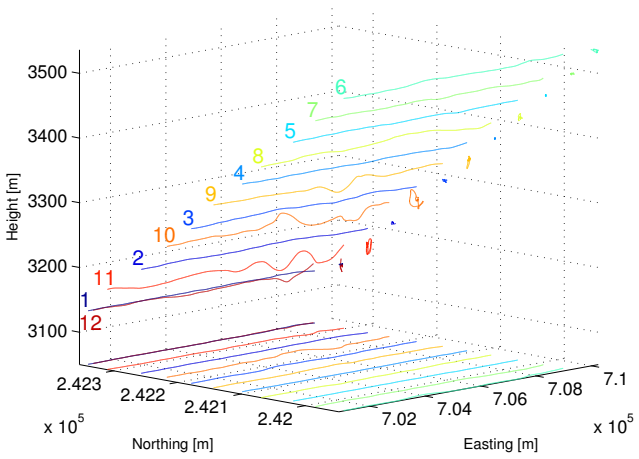

Fig. 1. P-band tomographic acquisition pattern consisting of 11 flight tracks + 1 control track. The flight direction is from east to west and the sensor is left-looking. In addition to the actual flight tracks, their projections to the horizontal plane and to the northing-height plane are depicted.

Carrier frequency	350 MHz
Chirp bandwidth	70 MHz
Sampling rate	100 MHz
Polarizations	HH-HV-VV-VH
PRF	500
Ground speed	90 m/s

TABLE I
E-SAR P-BAND SYSTEM PARAMETERS.

Number of flight tracks	11+1
Nominal track spacing d_n	56.6 m
Horizontal baselines	40 m
Vertical baselines	40 m
Synthetic aperture in normal direction L	566 m
Nominal resolution in normal direction δ_n	3 m
Approx. unambiguous height H	30 m

TABLE II
NOMINAL PARAMETERS FOR TOMOGRAPHIC PROCESSING.

which maps the volume at the position $\vec{r}_i$:

$$v(\vec{r}_i) = \sum_{k=1}^{m} \sum_{j=a_k(\vec{r}_i)}^{b_k(\vec{r}_i)} g_k(R_k, \vec{r}_{S_{jk}}) \cdot R_k \cdot \exp(i2k_c R_k) \ , \quad (2)$$

where m is the number of flight tracks that build the tomographic pattern. The boundaries of the synthetic aperture in azimuth direction, a_k and b_k, vary as a function of the grid position $\vec{r}_i$. This means that we sum up the contributions from those sensor positions $\vec{r}_{S_{jk}}$ which actually build the synthetic aperture for the grid position $\vec{r}_i$. Note that an appropriate interpolation procedure is required in order to retrieve the data values at the correct range distances because of the discrete representation of the range-compressed data.

III. EXPERIMENTAL SET-UP

An extensive airborne SAR campaign has been carried out in September 2006. Two fully polarimetric tomographic data sets - a P-band and an L-band data set - of a partially forested area have been acquired by the German Aerospace Center's E-SAR system. Eight corner reflectors were deployed for geometric and radiometric calibration purposes. The positions of the corner reflectors were measured by carrier-phase differential GPS. In the following, we restrict ourselves to describing the P-band data set as we have not evaluated the L-band data so far. In Table I the parameters of the E-SAR P-band system are summarized. Note that the reduced chirp bandwidth of only 70 MHz in the P-band is due to restrictions imposed by the Swiss Federal Office of Communications to prevent interference of the radar signal with existing RF communication services within the band 390-395 MHz. The nominal chirp bandwidth is 94 MHz for both L- and P-band. The 12 P-band data sets were acquired within one air mission. The maximal time span between the first and the last track is approx. 2 h. In Fig. 1 the geometric configuration of the flight tracks for the P-band tomographic data set is shown. The flight direction is from east to west and the sensor is left-looking. In addition to the actual flight tracks, their projections to the horizontal plane and to the northing-height plane are also depicted. The mission was completed by a control track which has the same nominal flight geometry as the first track. Table II contains a summary of the parameters which characterize the tomographic data set.

IV. SIMULATED DATA

In order to quantify the performance of the tomographic processing by TDBP two complete tomographic P-band raw data sets have been simulated and processed. The raw data simulator emulates the true 3D acquisition geometry using the navigation data of the actual flight tracks and the 3D position of a point target. The same system parameters have been used as given for the real P-band data acquisition. In Fig. 2 the tomographic slice in normal direction of a focused point target is depicted. Fig. 3 shows the focused signal of another simulated data set, where a second point target is added, separated from the first one by a distance of 12 m in the normal direction. And in Fig. 4 the tomographic slice in normal direction of an in-scene corner reflector is shown. The simulated data is based on exactly the same geometry as in the real situation. In all cases the point targets are focused properly in terms of resolution. But, the focused signal of the two simulated point targets aligned along the normal direction exhibits a rather strong ambiguous target detection and the focused signal of the corner reflector shows a considerable amount of anomalous side lobes. In addition, a slight mispositioning of the peak of the main lobe is present for the real P-band data.

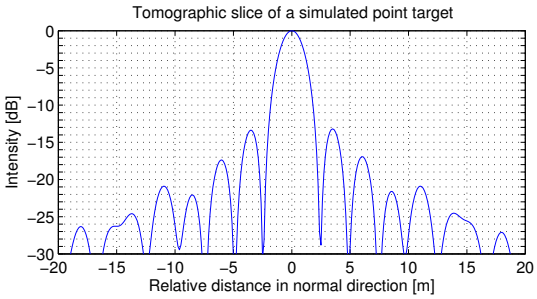

Fig. 2. TDBP tomographic imaging of a simulated multi-baseline P-band raw data of a single point target.

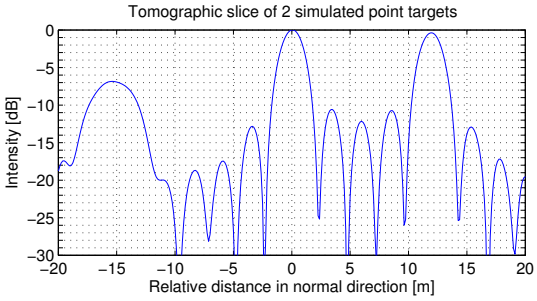

Fig. 3. TDBP tomographic imaging of a simulated multi-baseline P-band raw data set of two point targets which are separated by a distance of 12 m in normal direction.

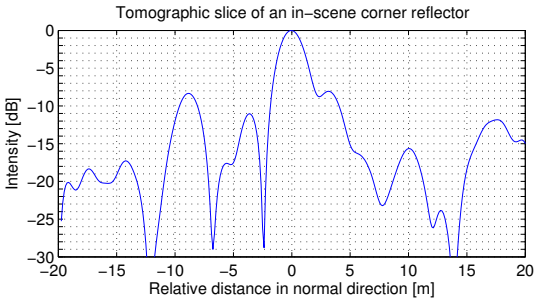

Fig. 4. TDBP tomographic imaging of an in-scene corner reflector of the real multi-baseline P-band data set.

V. Experimental Results

A partially forested area of 400 m x 1000 m size has been selected for tomographic processing using the HH channel of the P-band tomographic SAR data set. For simplicity, and since the selected area is relatively flat, a 3D reconstruction grid consisting of a set of horizontal layers has been chosen. The voxel spacing is 1 m for both, easting and northing direction, and 1.5 m in vertical direction. In Fig. 5 seven tomographic slices of the imaged volume are depicted. Three of them run in south-northern direction and the other four run in west-eastern direction. For smoother visualization the data have been upsampled in the vertical direction by a factor of 2 after focusing. The tomographic slices represent the measured radar intensity values in dB. The red and the green dashed lines indicate the height information taken from the laser DEM or DSM, respectively. In addition, a horizontal layer of the volume on the height level H = 551 m is shown as well as an orthorectified RGB image of the same area. The RGB image was taken from the same platform during the airborne laser scanning campaign in 2003.

VI. Discussion and Conclusion

A comparison of the tomographic slices resulting from the airborne P-band data set and the DEM/DSM obtained from laser scanning indicates that high intensity values are predominantly located at the ground level within forested areas (note that most of the deciduous trees are probably not included in the DSM due to laser data acquisition in early spring). This outcome conforms with what can be expected from horizontally polarized P-band radar back-scattering of a forested area, where double-bounce scattering from the ground surface and tree trunks is a dominant scattering mechanism. However, high intensity values are often accompanied by considerable side lobes and ambiguities in the normal direction. The simulations show that the point targets are well-focused by tomographic processing using the TDBP algorithm in terms of resolution and separability. However, if multiple targets are distributed along the normal direction the focused signal is disturbed by ambiguities as a result of the sparsely sampled synthetic aperture in normal direction. The slight mispositioning of the main lobe in the tomographic slice of the in-scene corner reflector and the rather high anomalous side lobes reveal a remaining inaccurate absolute geometric calibration of the data. So, first of all, a refined calibration with the help of the corner reflectors is needed. Then, a main focus will lie on investigating methods to suppress the ambiguities in combination with the TDBP processing approach.

Acknowledgment

The authors would like to thank Ralf Horn, Rolf Scheiber and Martin Keller at the German Aerospace Center (DLR) for their ongoing cooperation and technical support. They would also like to thank the procurement and technology center of the Swiss Federal Department of Defense (armasuisse) for funding and supporting this work.

References

[1] A. Reigber and A. Moreira, "First Demonstration of Airborne SAR Tomography Using Multibaseline L-Band Data," *IEEE Trans. Geosci. and Remote Sens.*, vol. 38, no. 5, pp. 2142–2152, 2000.

[2] F. Lombardini and A. Reigber, "Adaptive spectral estimation for multibaseline SAR tomography with airborne L-band data," in *Proc. IGARSS*, vol. 3, 2003, pp. 2014–2016.

[3] S. Guillaso and A. Reigber, "Polarimetric SAR Tomography (POLTOMSAR)," in *Proc. POLINSAR'05, Frascati, Italy*, 2005.

[4] F. Gini and F. Lombardini, "Multibaseline cross-track SAR interferometry: a signal processing perspective," *IEEE Aerosp. Electron. Syst. Mag.*, vol. 20, no. 8, pp. 71–93, 2005.

[5] M. Nannini and R. Scheiber, "A Time Domain Beamforming Algorithm for SAR Tomography," in *Proc. EUSAR, Dresden, Germany*, 2006.

[6] O. Frey, E. Meier, and D. Nüesch, "An integrated focusing and calibration procedure for airborne sar data," in *Proc. EUSAR, Dresden, Germany*, 2006.

[7] ——, "A Study on Integrated SAR Processing and Geocoding by Means of Time-Domain Backprojection," in *Proc. Int. Radar Symposium, Berlin, Germany*, 2005.

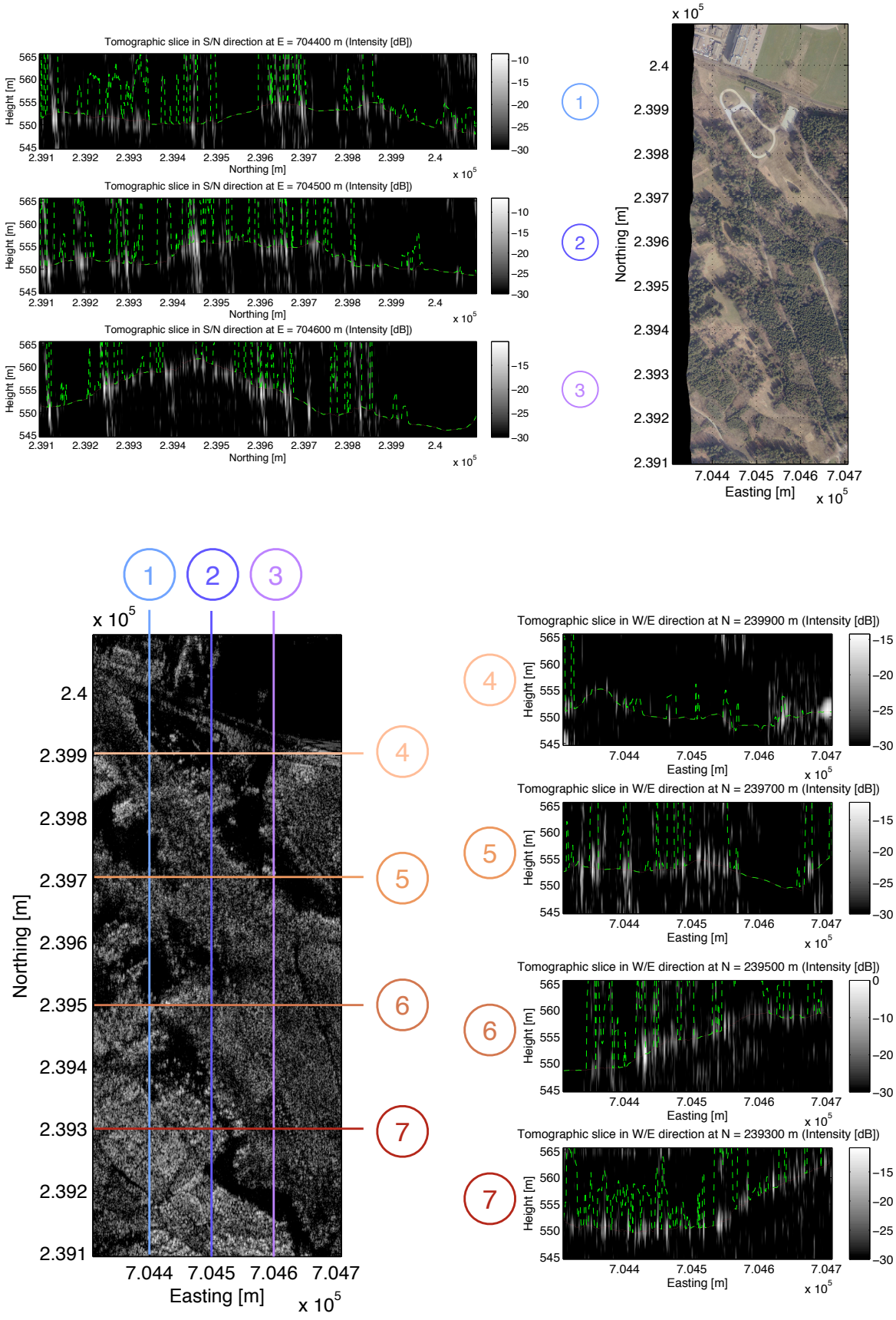

Fig. 5. Tomographic slices of a forested area derived from P-band HH E-SAR data. Upper left: tomographic slices in south-northern direction. Lower left: horizontal layer of the reconstruction grid on the height level H = 551 m . Lower right: tomographic slices in west-eastern direction. Upper right: RGB ortho-image of the same area. Red/green lines in the tomographic slices: DEM/DSM from airborne laser scanning (Falcon II, TopoSys GmbH).